

MDC H2683
JULY 1988

**SPACE -BASED SYSTEM DISTURBANCES CAUSED BY
ON-BOARD FLUID MOTION DURING SYSTEM MANEUVERS**

J. NAVICKAS

Presented to

1st National Fluid Dynamics Congress
Cincinnati, Ohio
24-28 July 1988

MCDONNELL DOUGLAS AERONAUTICS COMPANY-HUNTINGTON BEACH

MCDONNELL DOUGLAS

SPACE-BASED SYSTEM DISTURBANCES CAUSED BY ON-BOARD FLUID MOTION DURING SYSTEM MANEUVERS

J. Navickas*
McDonnell Douglas Astronautics Company
Huntington Beach, CA

Abstract

Disturbing forces and moments are calculated using the FLOW-3D finite difference code for a space-based oxygen tank under a suddenly applied settling acceleration for a case with a simultaneous liquid outflow and a case with no such outflow. Results show that the two conditions result in very different dynamic disturbances. The code accuracy is evaluated as part of the calculations and is shown to be adequate. Results also indicate that the storage tank geometry has a significant effect on the resulting disturbances.

Introduction

Many of the space-based systems currently in various design stages or proposed have rather complex mission requirements. In many of these missions, on-board propellant response to system dynamic disturbances can play a major role in mission success. Since long-duration experimental system performance verification in a low-gravity field may not be possible, computational methods may have to be used. To ensure the system design adequacy, two conditions must be satisfied: the computational accuracy of a chosen method must be evaluated and the critical operational conditions identified. In such an analysis it is usually necessary to predict the liquid-vapor configuration and the disturbing forces and moments applied to the system by the liquid motion.

Space Station will have a large number of fuel, life support, and other systems with large quantities of liquid on board, as will other space-based operations. Many of these systems will be delivered by the Shuttle, where safety considerations require the evaluation of dynamic Shuttle disturbances caused by fluid motion during boost, orbital payload ejection, and possible abort conditions. Such disturbances must be evaluated for single or multitank systems of various configurations. The ejection phase from the Shuttle payload bay can cause interference problems between the payload and the payload bay. The Centaur stage ejection from the Shuttle payload bay is perhaps the largest fueled stage that was to be ejected from the Shuttle payload bay.

The feasibility of such an ejection was studied experimentally and analytically by Aydelott, et al.¹ Experiments were conducted in the NASA Lewis Research Center test facility and the resultant gas bubble motion in a low gravity field compared to the motion computed with the NASA-VOF3D code. Martin² compared the NASA test data¹ to HYDR-3D³ program computations for the same Centaur oxygen tank. Der and Stevens⁴ have also conducted HYDR-3D computations of bubble motion in a low-gravity field. These comparisons indicate that the computed vapor volume deformations are similar to the experimental ones, suggesting that the code should predict the fluid-induced disturbances with reasonable accuracy. Estes, et al,⁵ compared the spacecraft fuel-induced forces and moments to experimental

ones measured in the NASA KC-135 aircraft flying a Keplerian trajectory. Computations were performed using a predecessor of the production HYDR-3D code. Computational results show reasonable agreement to test data.

After orbital injection, space-based systems can have a variety of operational environments. In some applications it is necessary to transfer fluids between space storage systems. The Space Station supply represents a family of such missions.

In the present analysis, oxygen tank fluid-induced forces and moments were computed for both flow and nonflow conditions using the FLOW-3D code,⁶ a current version of the HYDR-3D code. The purpose of the analysis was two-fold—to check the accuracy of the FLOW-3D code and to gain an understanding of the significant sources of disturbances under a likely operating envelope. In a related analysis Navickas and Ditter⁷ have shown that the tank configuration can have a significant effect on the resulting disturbances. This analysis was extended to show the effect of the initial vapor bubble location on such disturbances. The evaluation of the code accuracy in a flow system is especially important, since most of the FLOW-3D and related code evaluations were conducted with nonflow systems. The flow cases were structured to provide some indirect evidence of the code accuracy in such flow applications.

Computational Method

The FLOW-3D program is an outgrowth of the Marker-and-Cell programs.⁸ It has been under continuous development since the initial Marker-and-Cell version. Much of the effort has been concentrated on improving computational speed and accuracy. The program has also been greatly improved in input-output routines, computer graphics, and inputting of complicated solid-surface boundaries. Vehicle motion is user-supplied via a special routine reserved for that purpose. It can represent a general motion of a vehicle-fixed coordinate system with respect to an inertial coordinate system. Surface tension is added explicitly and wall shear is added implicitly. Separate computational routines are included to solve compressible, partially compressible, and incompressible flows. A system with one com-

pressible and one incompressible fluid with a common boundary can be computed. The computational grid consists of a specified number of zones with a specified number of nodes in each zone. When the smallest node in each zone is specified, the remaining node sizes increase progressively. Such an approach minimizes the effect of large nodes connected to small ones, a condition that can affect computational accuracy.

The solution proceeds by estimating explicitly the present time velocities from previous time step advective, pressure, and other accelerations. The pressures are then iteratively adjusted to satisfy the continuity equation. Each pressure adjustment requires an adjustment of the calculated velocities. This procedure is continued until desired convergence criteria are satisfied. Summation of forces and moments with respect to any set of arbitrary axes is done by integrating pressures over tank surfaces.

As the code evolved from the HYDR-3D to the FLOW-3D version, a capability to represent the vapor volume by a uniform pressure polytropic state, $pV^\gamma = \text{constant}$, was included, where p, V and γ are the vapor pressure, volume, and specific heat ratio, respectively.

Computational Results

A spherical oxygen tank 1.2 m in diameter was considered in the present analysis. In the no-flow condition the tank was exposed to a settling acceleration with a number of initial vapor-volume locations. Such an environment may represent a tank ejection from the Shuttle payload bay or an orbital fluid settling. In the flow case an unsymmetric initial liquid-vapor configuration was assumed with liquid outflow out of the tank together with a small settling acceleration level. Schematic diagrams of the two cases considered are shown in Figure 1.

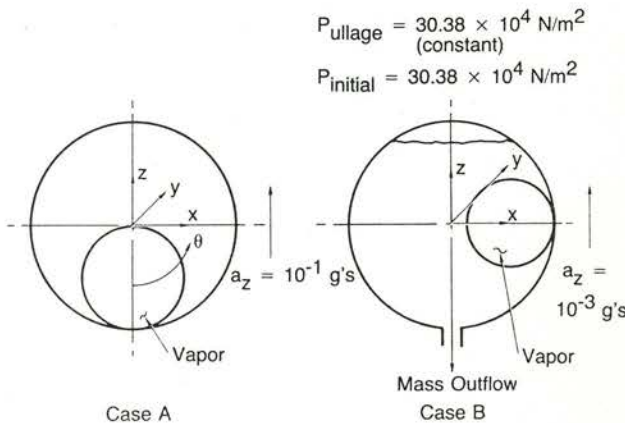


Fig. 1 Cases considered in fluid dynamic disturbance of the storage system

1. **No-Flow Condition.** The primary variable affecting the fluid dynamic response to external disturbances is the initial location of the ullage vapor volume, which must be determined to provide the proper initial conditions for the disturbance computations. As a possible scenario, it may be postulated that a vapor bubble drifts through the liquid volume after the payload is rotated out of the Shuttle payload bay. This drift is caused by low-level aerodynamic drag in

a low earth orbit. During this drift phase the bubble may assume a distorted spherical shape, the degree of distortion depending on the Bond number. Such a drift may take a considerable length of time. Eventually the bubble may come in contact with the tank sidewall or some internal tank structure. At this point the minimum energy configuration is no longer a spherical or spheroidal shape, but rather a flat interface. This can be shown to be the case from minimum energy considerations. To reach the minimum energy state, thermal or mechanical energy must be input. After an equilibrium bubble shape and location are reached, a variety of orbital maneuvers may disturb such an equilibrium position. Because of such influences, the initial liquid-vapor configuration prior to a maneuver may be difficult to determine.

For the purposes of the present analysis a spherical ullage vapor configuration was assumed. Three vapor bubble configurations were considered: bottom of the tank ($\theta = 0$ deg), side of the tank ($\theta = 90$ deg), and top of the tank ($\theta = 180$ deg). An acceleration level of 0.1 g's was applied at $t=0$ and forces and moments about a coordinate system located at the center of the tank were calculated. This is accomplished by integrating forces on the internal tank surface. A vapor bubble diameter of 0.6 m was assumed. A typical liquid-vapor configuration at $t=0.5$ sec for an initial bubble location at $\theta = 90$ deg is shown in Figure 2. The x-force magnitude is shown in Figure 3. The x-force magnitude for the initial bubble location at the top of the tank is shown in Figure 4. Since this is a symmetric condition, there should be no net force in this direction. This is one good check of the code computational accuracy and has been used extensively in the present study. The forces caused by computational limitations are rather small for this particular case. Moments about the y-axis are shown in Figure 5. Although there is a significant side force in the x-direction, the moments are negligible, indicating that the force acts essentially along the x-axis.

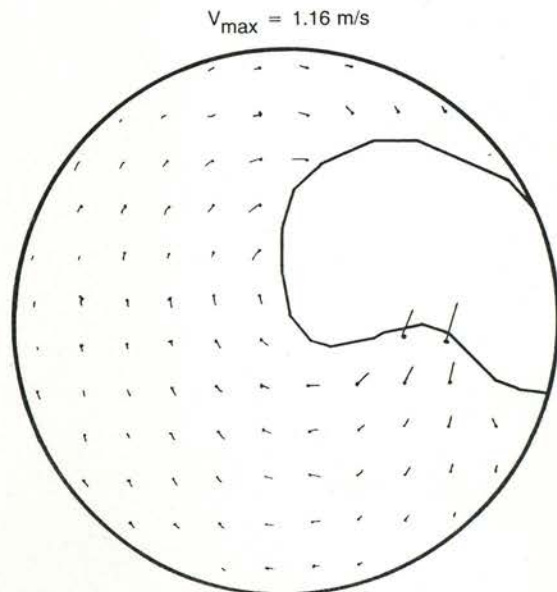


Fig. 2 Case A flow field characteristics, $t = 0.5$ sec, $\theta = 90$ deg

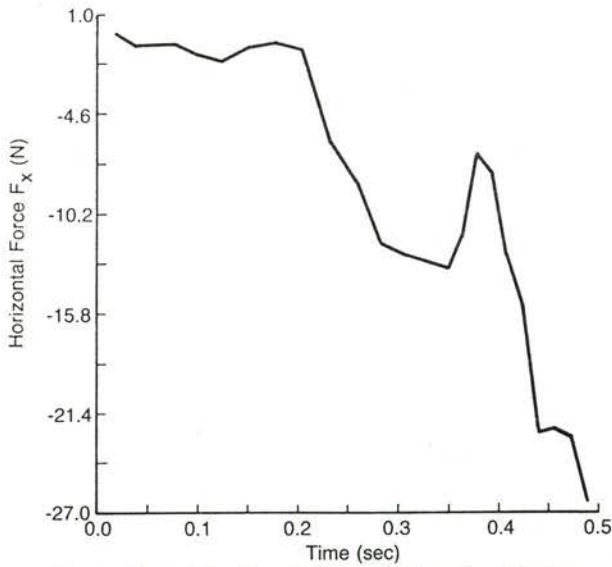


Fig. 3 Case A horizontal force history $\theta = 90$ deg

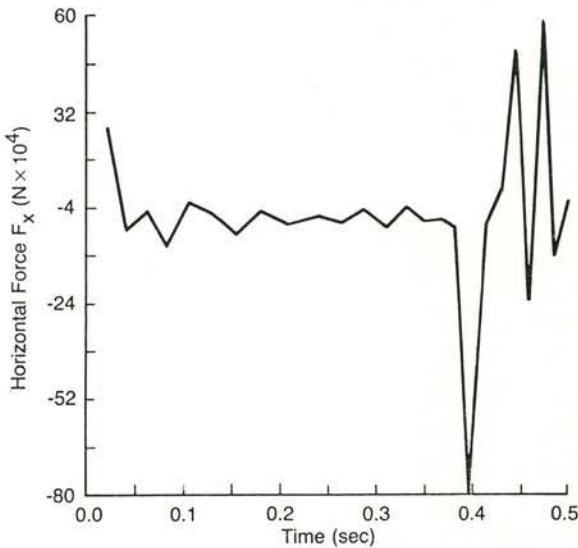


Fig. 4 Case A horizontal force history $\theta = 180$ deg

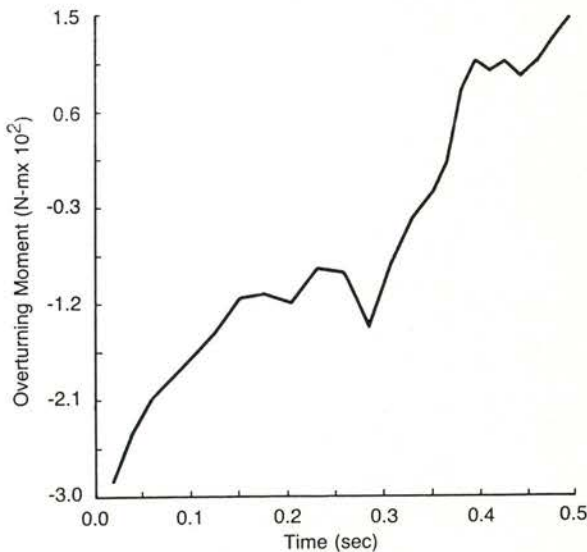


Fig. 5 Case A overturning moment $M_{y-y'}$, $\theta = 90$ deg

Forces along the longitudinal (z-axis) for the three vapor-volume configurations considered are shown in Figure 6. It is quite apparent that the vertical force is a very strong function of the initial liquid-vapor configuration. Such results suggest that the vapor bubble location must be carefully determined prior to a space-based maneuver in systems where overturning moments (moments about the x-x or the y-y axes) are critical. Where the certainty of such a determination cannot be ensured, a combination of liquid-vapor configurations in each tank must be assumed to give the largest overturning moment. Single spherical tank overturning moments are negligible if the vehicle center of gravity corresponds to the tank origin. For instance, if four fuel tanks are mounted on a circular ring, an initial bubble position at the top of one tank ($\theta = 180$ deg), and an initial bubble position at the bottom of a tank located 180 deg from the first tank on the mounting ring would result in the maximum overturning moment, which would be equal in magnitude to the difference in vertical forces, shown in Figure 6, multiplied by the moment arm.

For a single spherical tank, the overturning moment is negligible if the vehicle center of mass coincides with the tank origin, as shown in Figure 5. However, in designs where these points do not coincide, the overturning moment is equal to the force shown in Figure 3 multiplied by the appropriate moment arm. Such results suggest that the overturning moment can be minimized by a proper system design.

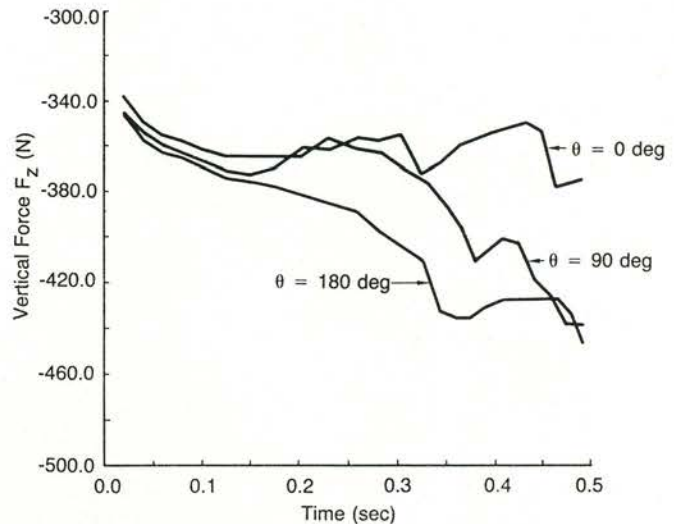


Fig. 6 Case A vertical force histories

2. Flow Condition. In the flow condition the tank was assumed to empty simultaneously with an applied settling acceleration of 10^{-3} g's. A constant initial pressure throughout the system and a constant ullage pressure during the outflow process and a bubble diameter of 0.5 m were assumed. The tank was assumed to reach the maximum outflow rate in 0.02 second. Values of $\gamma = 1.4$ (adiabatic) and $\gamma = 1$ (isothermal) were used in the computations. Initial vapor bubble at the extreme x-axis location ($\theta = 90$ deg) was assumed. A case with the bubble at the center of the tank was also considered to evaluate the code computational accuracy, since this condition should result in no net force in the x or y direction.

The tank-emptying condition resulted in an oscillating force in the x-direction, as shown in Figure 7, for cases of $\gamma = 1.4$ and $\gamma = 1.0$. Since the model considered is essentially a spring-mass system, it shows different oscillating frequencies for the two γ values considered. The $\gamma = 1.4$ condition represents a "stiffer" spring with the resulting higher frequency of oscillation. The magnitude of the side force is also a strong function of the mass outflow rate. The net force in the y-direction is shown in Figure 8 as an indication of the program computational accuracy. Errors of similar magnitude were obtained for the case with centrally located bubble. Unlike the unsymmetric bubble case, results show no net x-force oscillation for the centrally located bubble. Because of symmetry, there should be no such force. Velocity vectors for the $\gamma = 1.4$ case at $t = 0.62$ sec and $t = 0.64$ sec are shown in Figures 9 and 10, respectively. Figure 9 represents a contracting bubble volume and Figure 10 an expanding one. The bottom of the tank is not shown, since the scaling of the large outflow velocity vector would reduce the depiction of the remaining velocity vectors to mere dots. Inspection of both figures indicates a developing interface stability failure at the upper portion of the bubble. A large down velocity is developed at one node of the interface during the decreasing bubble size phase and persists during the expanding phase while the velocity of the adjacent node

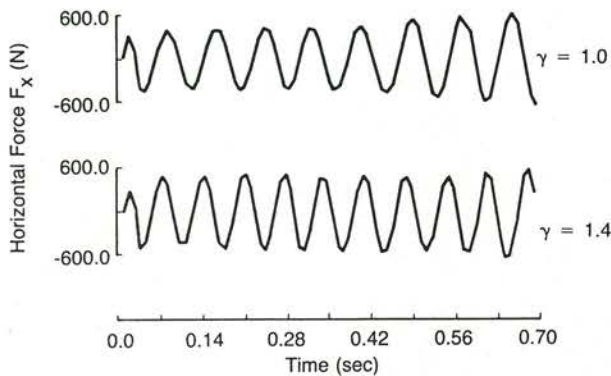


Fig. 7 Case B horizontal force during outflow

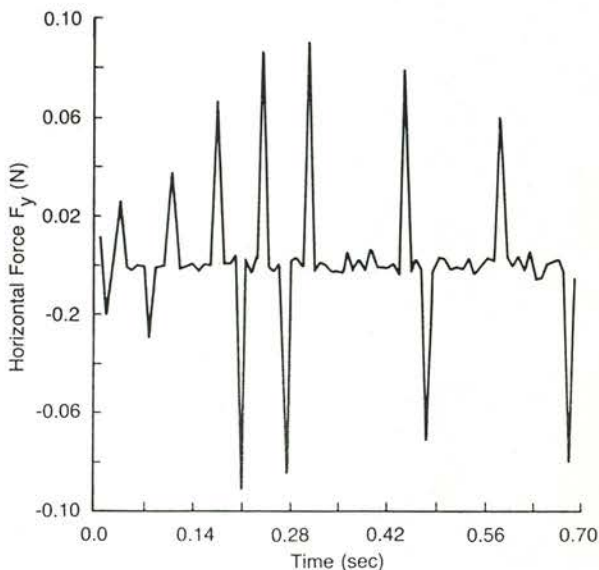


Fig. 8 Case B horizontal force history, $\gamma = 1.4$

changes direction. The rather complex response of an emptying fluid storage system with an imbedded large ullage volume in the liquid bulk suggests that every design where such a condition can exist should be evaluated with the proper input parameters, such as the tank geometry, vapor volume, pressure, outflow rate, etc. Where such disturbances are a source of potential operational problems, steps can be taken to minimize these disturbances.

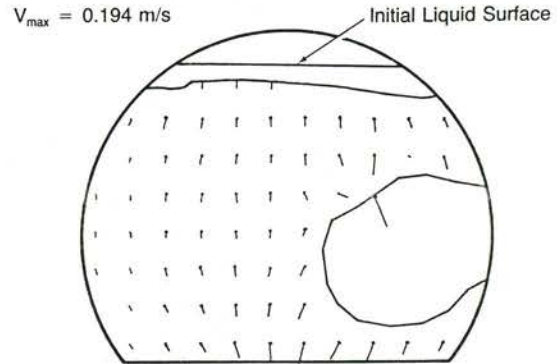


Fig. 9 Case B velocity vectors, $\gamma = 1.4$, $t = 0.62$ sec

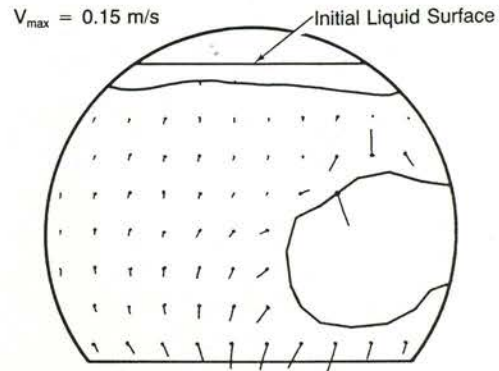


Fig. 10 Case B velocity vectors, $\gamma = 1.4$, $t = 0.64$ sec

Conclusions

Finite-difference computational methods that can track large liquid surface displacements during system dynamic disturbances can be a useful tool in the design of space-based fluid storage systems of complex geometries. One such program, FLOW-3D, was evaluated under a variety of dynamic conditions to check the program accuracy and identify possible critical design conditions. A space-based oxygen tank under a suddenly applied settling acceleration with both mass outflow and no mass outflow conditions was considered. Results indicate very different dynamic disturbances created by the two chosen conditions. Results also show that a proper choice of the fluid storage system geometry can minimize system dynamic disturbances, implying that available finite-difference computational methods should be used in the design of space-based fluid storage systems.

References

1. J. C. Aydelott, et al, Numerical Modeling of On-Orbit Propellant Motion Resulting from an Impulsive Acceleration, Paper AIAA-87-1766, AIAA/SAE/ASE/ASEE 23rd Joint Propulsion Conference, San Diego, California, 19 June-2 July 1987.
2. R. E. Martin, Effects of Transient Propellant Dynamics on Deployment of Large Liquid Stages in Zero-Gravity with Application to Shuttle/Centaur, Paper 86-119, 37th International Astronautical Congress.
3. J. M. Sicilian and C. W. Hirt, HYDR-3D, A Solution Algorithm for Transient 3D Flows, Flow Science, Inc., Report FSI-84-00-2, August 1984.
4. J. J. Der and C. L. Stevens, Low Gravity Bubble Reorientation in Liquid Propellant Tanks, Paper AIAA-87-0622, AIAA 25th Aerospace Sciences Meeting, Reno, Nevada, 12-15 January 1987.
5. T. W. Estes, et al, Zero-Gravity SLOSH Analysis, ASME 1985 Winter Annual Meeting, Miami, Florida, 1985.
6. FLOW-3D, Computational Modeling Power for Scientists and Engineers, Flow Science, Inc., Technical Manual.
7. J. Navickas and J. Ditter, Effect of the Propellant Storage Tank Geometric Configuration on the Resultant Disturbing Forces and Moments during Low-Gravity Maneuvers, ASME Winter Annual Meeting, Boston, Massachusetts, 13-18 December 1987.
8. J. E. Welch, et al, The MAC Method: A Computing Technique for Solving Viscous, Incompressible, Transient Fluid-Flow Problems Involving Free Surfaces, Los Alamos National Laboratory Report LA-3425, 1966.